Colloid Polym Sci (2006) 284: 611–619
DOI 10.1007/s00396-005-1405-3

ORIGINAL CONTRIBUTION

Viktória Hornok
András Erdőhelyi
Imre Dékány

Preparation of ultrathin membranes by layer-by-layer (LBL) deposition of oppositely charged inorganic colloids

Received: 5 April 2005
Accepted: 30 August 2005

V. Hornok · I. Dékány (✉)
Department of Colloid Chemistry,
Nanostructured Materials Research
Group of the Hungarian Academy
of Sciences, University of Szeged,
Aradi Vértanúk tere 1,
6720 Szeged, Hungary
E-mail: i.dekany@chem.u-szeged.hu

A. Erdőhelyi
Department of Solid State
and Radiochemistry, University of Szeged,
Aradi Vértanúk tere 1,
6720 Szeged, Hungary

Abstract Nanofilms were prepared by alternating deposition of Mg–Al (2:1) NO_3^- layered double hydroxide (LDH), hectorite and silica particles present study. The charge density of the oppositely charged materials strongly affect film properties like thickness and ordering. The specific charge of the colloidal particles was measured with the particle charge detector. The sequential build up of the thin films was followed by spectrophotometry and X-ray diffraction (XRD). The surface morphology of the formed multilayers was characterized and film thickness determination was performed by atomic force microscopy. The influence of the charge density of hectorite and silica particles on the LDH/hectorite, LDH/silica film thickness was studied. The results reveal that the LDH concentration has a significant effect on the film thickness while the hectorite and silica concentration were not important. Films prepared from the different types of negatively charged inorganic particles in the same concentration range (0.25–1.0%) have similar thickness because of the much higher surface charge relative to the LDH lamellae.

Keywords Layered double hydroxides · Membranes · Multilayers · LBL method

Introduction

The sequential film preparation technique was developed by R. K. Iler in 1965 to form films of controlled, uniform thickness from charged colloidal particles [1]. This universal method bases on the Coulomb attraction between the oppositely charged particles and has gained widespread application [2–10]. The deposition may be carried out by at least three different ways, namely solution dipping, spraying or spin coating. The application of layers by spraying was introduced by Schlenoff et al. [11] and the use of spin-coaters was demonstrated by Hong and also Wang [12–14]. Preparation of ultrathin membranes formed from charged colloidal particles by sequential solution dipping is used in this study. Numerous studies have been published in the field of nanofilm preparation with polymers [15–17]. Recent work demonstrates film preparation by using inorganic materials like LDH, hectorite, and silica particles. Films prepared from these materials are potential gas separation systems while the size of discontinuities in nanostructured materials make them able to separate different particles by filtration [18–23]. Polymer/layered silicate multilayer films were already prepared by the layer-by-layer method [24–26]. The polymer layers order the nanothin silicate lamellae at any plane surface (glass or polymer) [24, 25]. Positively charged octahedral sheets separated by exchangeable anions (Cl^-, NO_3^-, CO_3^{2-}, SO_4^{2-}) and water molecules constitute the layered double hydroxides. The general formula of the LDHs are: $[M^{2+}_{1-x}M^{3+}_x(OH)_2]^{x+}\ (A^{n-})_{x/n}\cdot yH_2O$, where M^{2+} can be Mg^{2+}, Fe^{2+}, Co^{2+}, Ni^{2+}, Zn^{2+} and M^{3+} may be Al^{3+}, Cr^{3+}, Fe^{3+}, Co^{3+} [27, 28]. The properties of LDHs, particle size and specific area depend on the way of preparation, type of consisting ions and the amount of exchangeable anions [26]. These materials gain widespread applications such as air and water purification, catalysts in the production of intermediates and fine chemicals [29, 30], in various hydrogenating processings. Surprising and promising experiments were performed in applying LDH in photochemistry, medicine and enviromental chemistry [31].

Materials and methods

The hydrotalcit type LDH (Mg:Al = 2:1) was prepared from alumina nonahydrate ($Al(NO_3)_3 \cdot 9H_2O$) and magnesium nitrate hexahydrate ($Mg(NO_3)_2 \cdot 6H_2O$). Two solutions were prepared: Mg^{2+} and Al^{3+}-nitrate in boiled off distilled water—solution A and $NaNO_3$ and NaOH dissolved in boiled off distilled water—solution B. Solution B was added to solution A dropwise and was stirred for 5 h in N_2 atmosphere at 60 °C. After that the dispersion was left at ambient temperature (under N_2), the LDH particles were separated by ultracentrifugation, washed with distilled water and dried at 65 °C. The powdered sample was characterized by X-ray diffraction.

Synthetic sodium hectorite (Süd-Chemie AG, Germany) and colloidal silica particles of LUDOX silica sol (Du Pont, $d = 15.6$ nm measured by Malvern Zetasizer dynamic light scattering method) were applied as the negative component in film preparation. The LDH dispersion of 0.5 and 1% (g/100 cm^3) and 0.25, 0.5 and 1% of the hectorite dispersion or silica sol were used. The nanofilms were prepared on cleaned Menzel Superfrost glass (Fischer Sci. Co.) by layer-by-layer deposition method.

The charge of the colloidal particles were determined by measuring the potential in the particle charge detector (PCD) (Mütek Analytic GmbH, Germany). Hexadecylpyridinium chloride (HDPCl) was used to determine the specific charge of the negatively charged silica and hectorite particles. Light absorbance of the films was followed by Uvikon 930 UV–Vis two-way spectrophotometer. The absorbance after every dipping cycles were recorded. For representation, the $\lambda = 400$ nm data were used and the results were corrected by the absorbance of cleaned glass slide. X-ray diffraction measurements (XRD) were performed in a goniometer (Philips PW 1820, CuK_α, 40 kV, 30 mA, Ni grids as filter). The basal spacing was derived from the basal reflections (001).

The morphology of prepared films was characterized by Atomic Force Microscope Nanoscope III type Digital Instruments, USA, scanner with a piezo (scanning capability of 12.5 μm in *x*- and *y*- direction and 3 μm in *z*-direction). A tapping type tip made of silicon was used (Veeco Nanoprobe Tips RTESP modell, 125 μm length, 300 kHz). The film thickness was evaluated by measuring the difference between the mean height of the film related to the glass surface revealed by a scratch [32].

The nanofilms were prepared on glass surfaces by the layer-by-layer immersion technique. Prior to film preparation the glass slides were cleaned in chromic acid for hours to remove all the contamination, washed with distilled water and dried. The glass surface is negatively charged and forms thin films with positively charged particles. The glass slides were immersed into the LDH-dispersion for 10 min to form an LDH multilayer. This procedure must be followed by rinsing with distilled water in order to remove the weakly adhered particles (Fig. 1a). Aggregate formation on the surface is thus avoided. As a result, a thin LDH monolayer forms on the surface (Fig. 1a). The positively charged surface of the LDH film then binds negatively charged hectorite particles when immersed into the hectorite dispersion (Fig. 1b) or the silica sol (Fig. 1c). The immersion period took 10 min followed by half a minute rinsing with distilled water and drying with N_2.

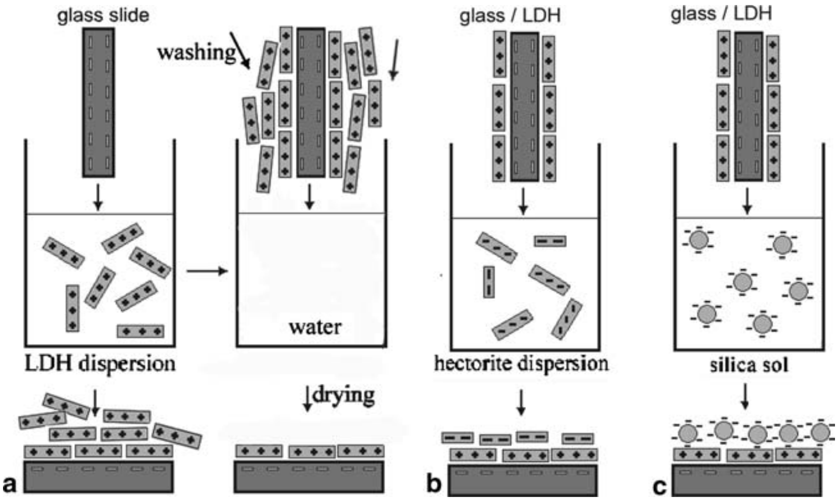

Fig. 1 Nanofilm preparation by the layer-by-layer immersion technique. **a** LDH films; **b** LDH/hectorite; **c** LDH/silica films

Results and discussion

LDH/hectorite and LDH/silica nanofilm series with different composition were produced. The specific charge of hectorite and silica particles was about 0.50 mequ/g and 0.12 mequ/g (Table 1) according to charge titration with 0.1% cationic surfactant (HDPCL) [33–35]. The HDPCl-hectorite and silica ratios at the equivalence points are also drawn in Table 1. The results of charge titration experiments of LDH dispersions with the oppositely charged hectorite and silica dispersion are also indicated in Table 1. Both cases 10 cm^3 of 1% LDH was titrated with the dispersions. It is obvious from the charge compensation point that 1.6 cm^3 of 0.1% hectorite dispersion is enough to compensate the charges of 100 mg LDH. In the case of silica—at the same concentration—2.66 cm^3 silica sol is necessary to compensate the LDH charges. The specific charge of LDH was obtained to 8.00×10^{-3} for hectorite and 7.98×10^{-3} meq/g for silica because the accessibility of the spherical silica nanoparticles and lamellar layer silicates are nearly the same on the external surface of LDH lamellae packages (Table 1).

In order to gain information about the interaction between hectorite, LDH and silica, charge equivalent amounts of hectorite dispersion and silica sol were added to LDH dispersions. After coagulation, the precipitates were filtered, dried and characterized by XRD (Fig. 2). The Bragg reflection at $d = 5.3$ nm characteristic of the composite and this peak indicates that aggregates of LDH and hectorite layers have been formed in the bulk suspension.

To prepare the LBL films from inorganic colloid particles 10 cycles of LDH/hectorite and LDH/silica nanofilms were prepared with 0.5 and 1% concentrations of LDH dispersions. The results of absorbance measurements demonstrate the sequential build up of the films from layer-to-layer (Fig. 3a–c). The absorbance

Table 1 Results of charge titration and charge equivalent point (ch.e.p.) determination

Titration with cationic surfactant HDPCl

Negatively charged sample	m (mg)	m_{HDPCl} ^{a} (mg)	ch.e.p. (g_{HDPCl}/g)	Specific charge of hectorite or silica (mequ/g)
Hectorite	15	2.677	0.178	0.50
Silica sol	15	1.626	0.108	0.30

Titration of LDH suspension with hectorite and silica

		m_{LDH} (mg) in suspension	ch.e.p. (g_{LDH}/g)	Specific charge of LDH (mequ/g)
Hectorite	1.60	100	62.5	8.00×10^{-3}
Silica sol	2.66	100	37.6	7.98×10^{-3}

ch.e.p., charge equivalent amount of added coagulant/g silica
^{a}Calculated from charge titration volume of HDPCl

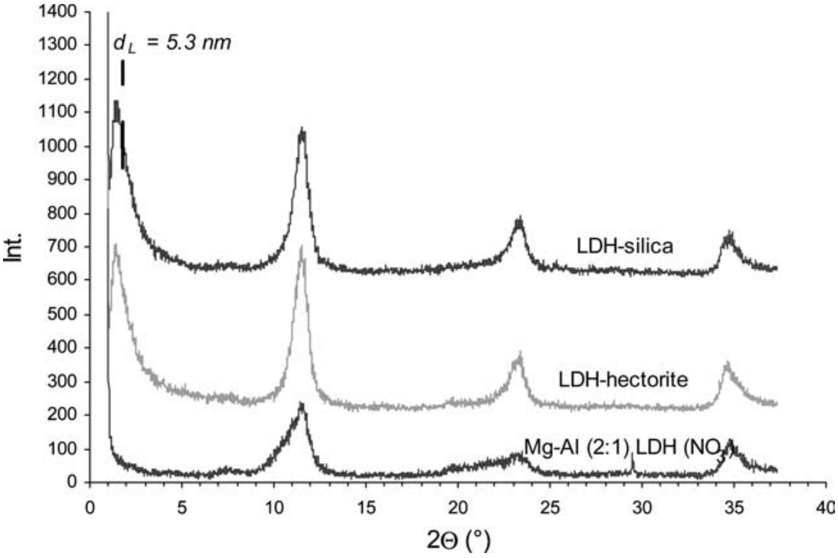

Fig. 2 XRD patterns of LDH, LDH/hectorite and LDH/silica composites

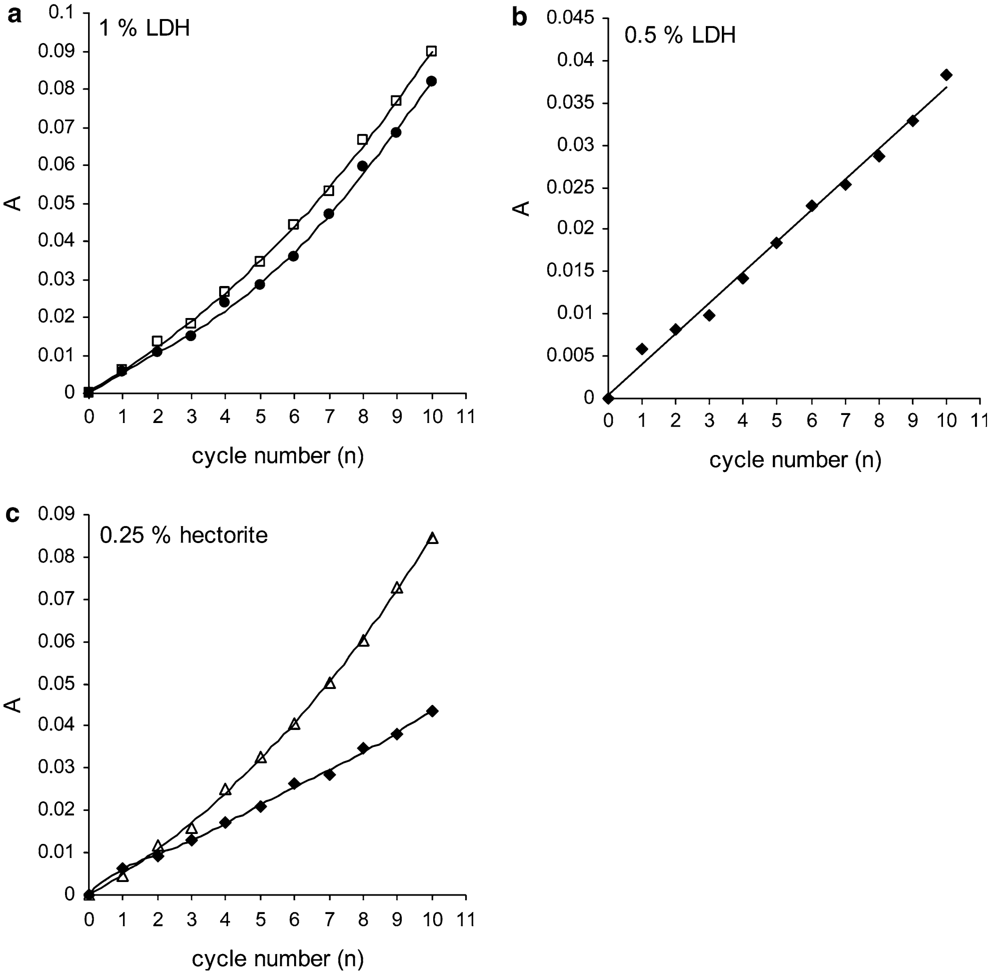

Fig. 3 Absorbance measurements of LDH/hectorite films ($\lambda = 400$ nm). **a** deposition of 1% LDH dispersion with (*open square*) 0.5% and (*filled circle*) 1% hectorite dispersion; **b** deposition of 0.5% LDH dispersion with 0.5% hectorite dispersion; **c** deposition of (*open triangle*) 1% LDH dispersion and (*filled diamond*) 0.5% LDH dispersion with 0.25% hectorite dispersion

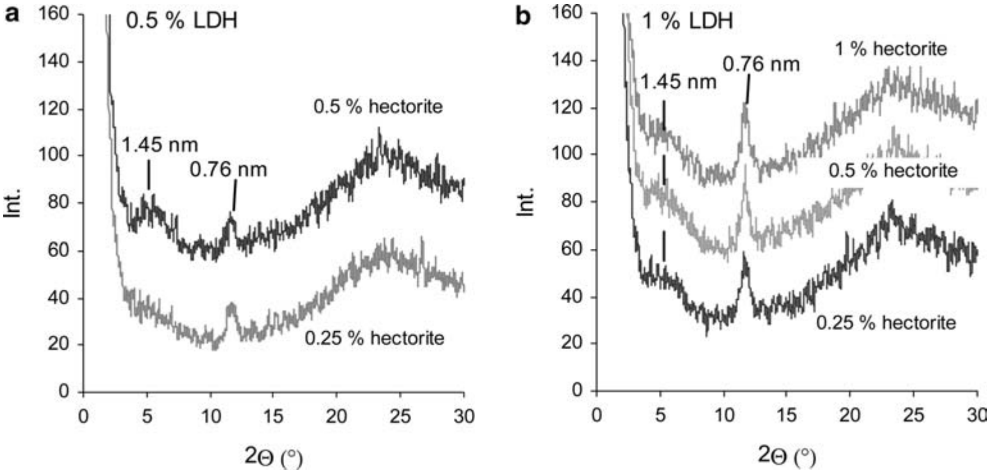

Fig. 4 XRD patterns of LDH/hectorite nanofilms. **a** deposition of 0.5% LDH dispersion at different hectorite concentrations, 10 cycles; **b** deposition of 1% LDH dispersion at different hectorite concentrations, 10 cycles

varied between 0.0045 and 0.089 ($\lambda = 400$ nm). The LDH-content has a significant effect on the absorbance while the hectorite concentration does not influence it. At given LDH concentration the absorbance curves do not show significant difference (Fig. 3a). The difference in LDH-content significantly influences the absorption at a given hectorite concentration (Fig. 3c). The absorbance of films prepared from 0.5% of LDH increased

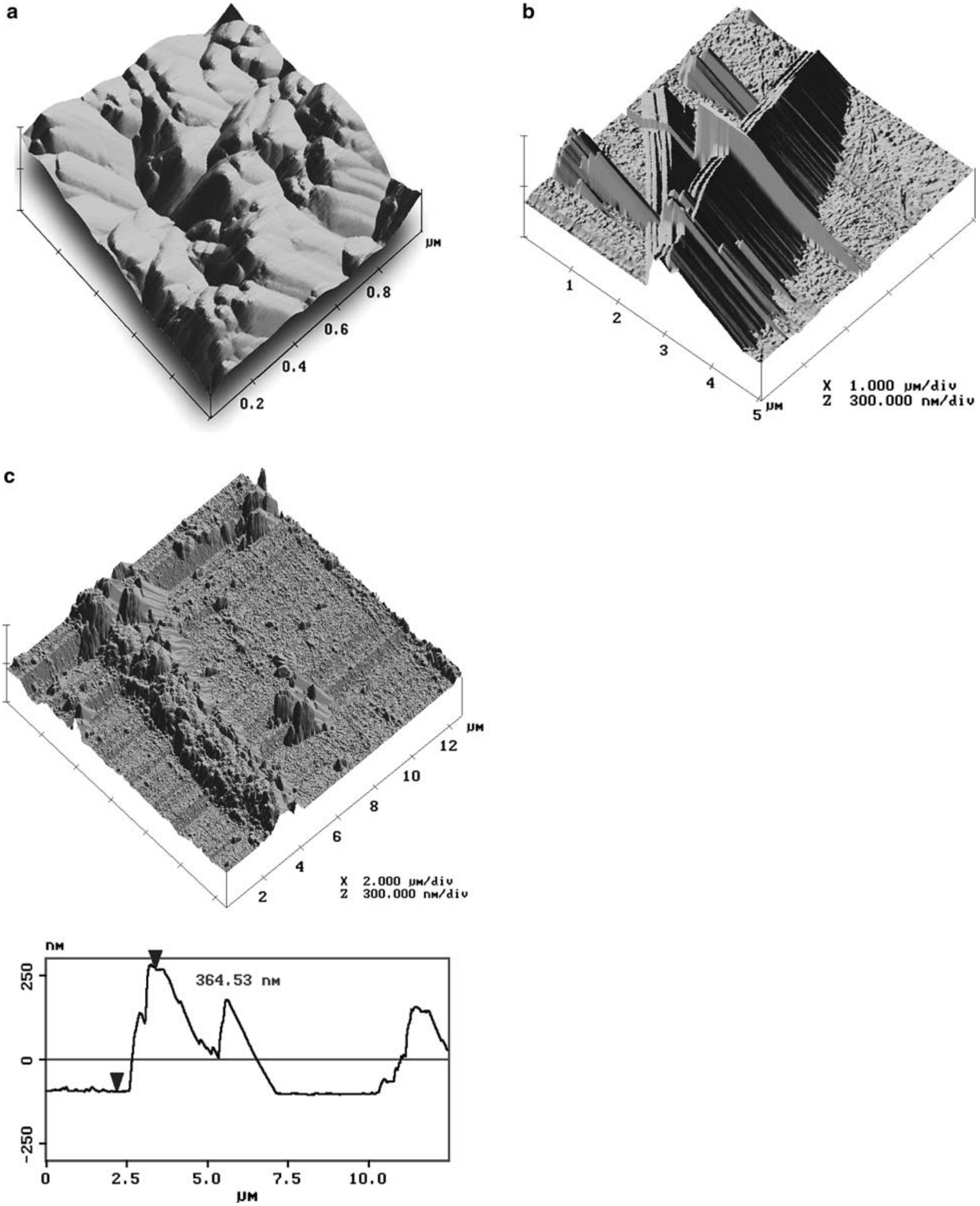

Fig. 5. AFM images of LDH/hectorite multilayers. **a** 0.5% of LDH and 0.5% of hectorite at $n = 10$; **b**, **c** film thickness determination with AFM

Table 2 Absorbance and specific deposited amount of different LBL films (at $n=10$ cycle)

Type of film	A (at $\lambda=400$ nm)	Specific deposition (mg/cm^2)	Calculated layer thickness (nm)
1% LDH–1% hectorite	0.0820	0.315	747
1% LDH–0.5% hectorite	0.0897	0.345	817
1% LDH–0.25% hectorite	0.0846	0.326	771
0.5% LDH–0.5% hectorite	0.0384	0.188	349
0.5% LDH–0.25% hectorite	0.0436	0.214	397
1% LDH–1% silica sol	0.0898	0.346	822
1% LDH–0.5% silica sol	0.0866	0.333	792
1% LDH–0.25% silica sol	0.0823	0.317	753
0.5% LDH–0.5% silica sol	0.0469	0.181	430
0.5% LDH–0.25% silica sol	0.0472	0.181	431

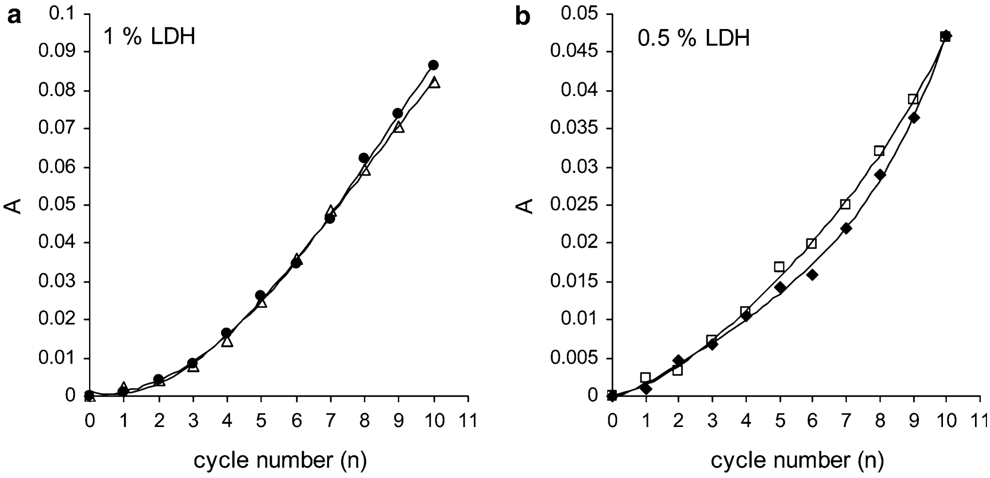

Fig. 6 Absorbance measurements of LDH/silica films ($\lambda=400$ nm). **a** deposition of 1% LDH dispersion with (*filled circle*) 0.5% and (*open triangle*) 0.25% silica sol; **b** deposition of 0.5% LDH with (*open square*) 0.5% and (*filled diamond*) 0.25% silica sol

linearly with cycle number. Due to the higher charge density at higher LDH content the LDH lamellae are capable to bind more hectorite lamellae and after a few cycles the aggregated and the not well-ordinated hectorite particles ensure higher surface for the next positively charged layer. The adhesion forces are increasing with increasing layer number in this composite structure.

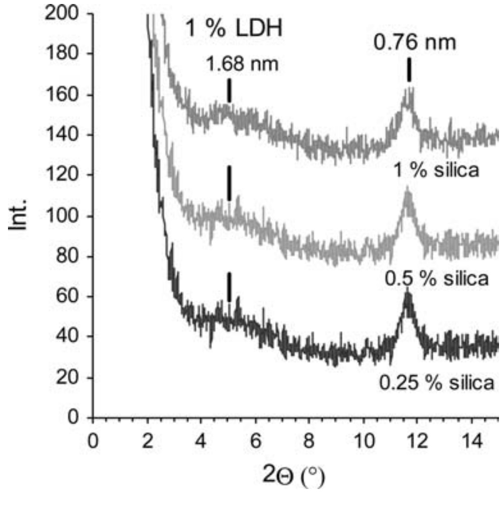

Fig. 7 XRD patterns of LDH/silica nanofilms. **a** deposition of 1% LDH dispersion at different silica concentrations, 10 cycles

The XRD patterns of LBL films prepared from 10 LDH/hectoliter cycles (Fig. 4) show a reflection of a basal spacing of 1.45 nm. The observed spacing may be related to the two-water layer structure of hectoliter stabilized by some magnesium and aluminum ions of the LDH or can be explained by the average *d*-space of interstratified single LDH and hectoliter layer. The reflection becomes more intensive for the dispersion of LDH was more concentrated while an effect of hectoliter concentration was not visible. The reflection intensities were distinctly smaller than the corresponding polymer films (as shown in our previous study).

The atomic force microscopy (AFM) images of 10 LDH/hectoliter cycles (1 μm×1 μm, Fig. 5a) illustrates the lamellar structure of hectoliter built up with distances of about 40–100 nm distance that denotes presence of hectoliter aggregates. To determine film thickness with AFM a new method was applied. The structure of the film was interrupted by scratches. At the area where the film is divided by the cutting line was imaged and we see the layered structure of the LDH/

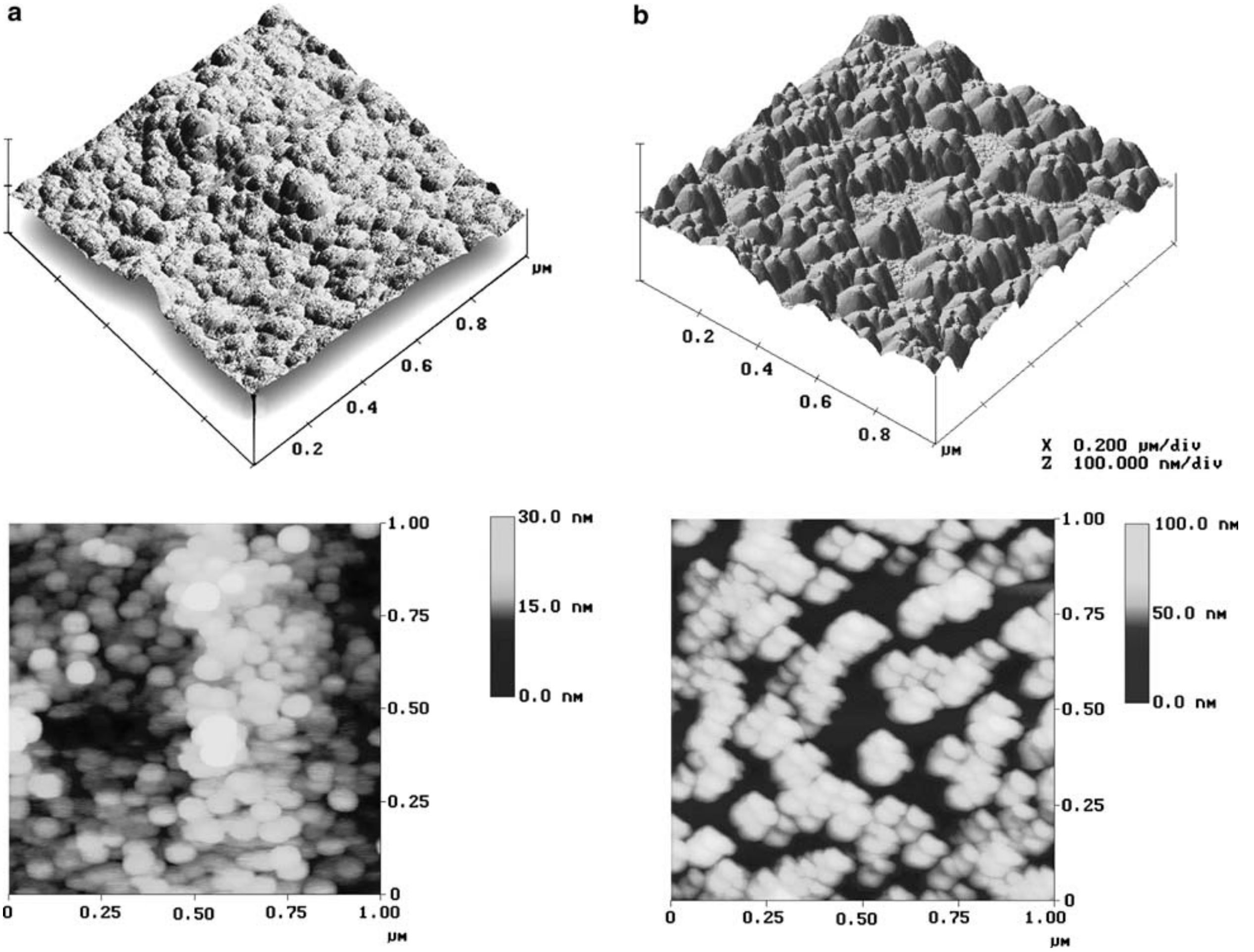

Fig. 8 AFM images of silica layers. **a** 0.25% of silica sol at $n=1$; **b** 0.1% of silica sol at $n=1$

hectorite composite (Fig. 5b). This procedure is a promising route to determine the film thickness and to compare it with the data calculated by absorbance measurements (Table 2). Figure 5c shows the cutting profile of the film and the thickness determined from the step height is 364 nm and this value shows good agreement with the 349 nm calculated from absorbance (Table 2).

Absorbance results of LDH/silicate films are similar to films discussed earlier i.e. the LDH concentration has a significant effect on the film thickness while it was practically not influenced by the silica concentration (Fig. 6a, b).

The presence of LDH was indicated by XRD by the reflection $d=0.76$ nm ($2\Theta=11.7°$). The intensity was practically independent on the silica sol concentration (Fig. 7). A broad maximum appeared at about $d=1.68$ nm ($2\Theta=4.5°$). The basal spacing of $d_L=1.68$ nm is characteristic of the silica/LDH intercalation where the small silica particles (about 1 nm) as pillars stick the LDH lamellae together.

AFM images (1 µm×1 µm) of LDH/silica films are presented in Fig. 8. Silica sol of 0.25% was examined after one cycle (Fig. 8a). The characteristic globular shape of the silica particle is well illustrated, the particles cover the surface completely. With the diluted (0.1%) sol (Fig. 8b) the surface was not completely covered but showed island-like arrangements of the particles.

To compare LDH/hectorite and LDH/silica films, absorbance data were studied. The dependence on the number of cycles are demonstrated in Fig. 9a. In the case of hectorite, thicker films are obtained and the curve is almost linear. The specific deposited amount in Table 2 was calculated from the absorbance data with the help of a calibration curve (see Appendix). The dependence of this amount on the number of cycles in case of silica at different LDH concentrations is shown in Fig. 9b and that for silica at different LDH concen-

Fig. 9 **a** Absorbance measurements of (*filled triangle*) 1% LDH/0.25% hectorite and (*filled circle*) 1% LDH/0.25% silica; **b** specific deposited amount of LDH/hectorite; **c** and for LDH/silica at different LDH concentration: (*filled square*) 0.1% LDH and (*filled diamond*) 0.5% LDH

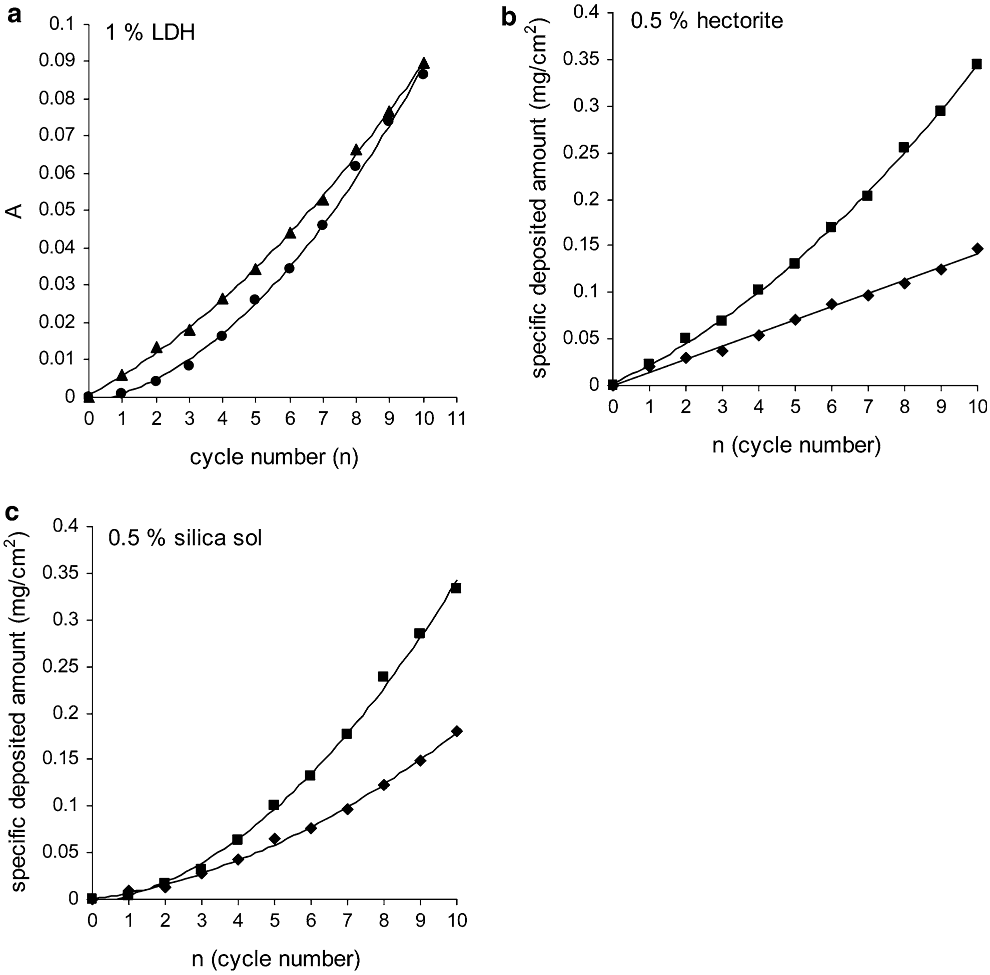

trations in Fig. 9c. The LDH concentration has a significant effect on the thickness, while the type of the negatively charged particle is not so important concerning the film thickness.

Conclusions

Nanofilms composed of LDH particles combined with hectorite and silica particles were prepared. Light absorbance, X-ray diffraction and AFM measurements were performed to obtain information about nanofilm properties, structure and morphology. As the charge density of hectorite is higher than that of silica, somewhat thicker films were formed in the presence of hectorite. The absorbance and thickness of the films increased with the number of cycles. X-ray diffractograms suggest that heterocoagulation occurs between the two inorganic oppositely surface charged particles. The film thickness data were calculated from absorbance values and were also determined by AFM. The surface profile of the cut film was imaged and the film thickness values derived from the two different methods showed good agreement.

Acknowledgements The authors wish their thanks Prof. Dr. Gerhard Lagaly for the valuable discussions and for the finantial support of the Hungarian Scientific Fund (OTKA) T 043430, M 045609 and for the Ministry of Education NKFP 03/047/2001.

Appendix

The spectra of applied materials were recorded to support that only the LDH determines the light absorbance of the films. The absorbance of hectorite dispersion and silica sol is negligible according to Fig. 10.

In order to determine film thickness a calibration curve of absorbance of LDH-dispersion with different concentrations (1–3%) was recorded. The measurements

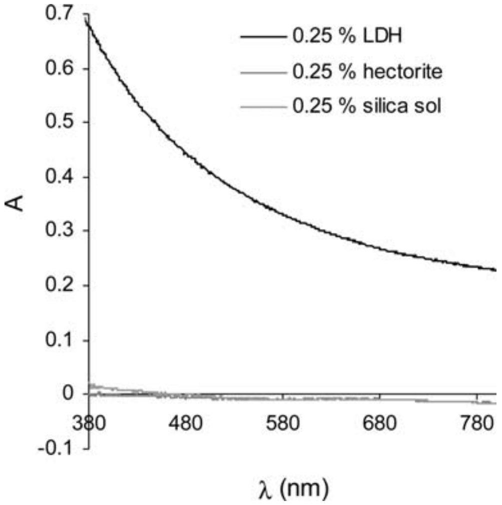

Fig. 10 Absorbance versus wavelength spectra of LDH, silica and hectorite dispersions

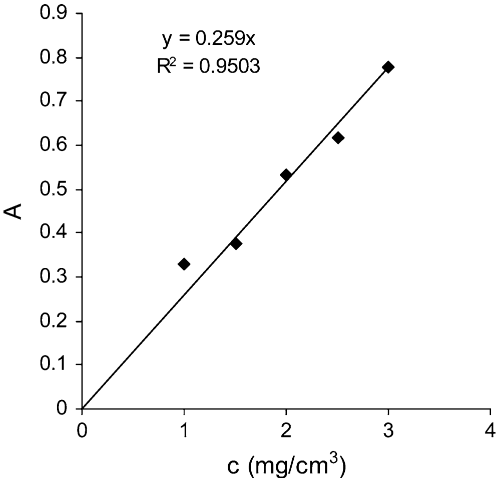

Fig. 11 Absorbance as function of LDH concentration in aqueous suspension

were performed at λ = 400 nm (Fig. 11). A calibration curve of this kind is acceptable in case of dispersions. In view of absorbance of films the amount of LDH on the glass surface can be determined on the basis of the calibration curve. This calculated value is called specific deposited amount and is in mg/m^2 dimension. The film thickness was calculated from the deposited amount divided by the density of the film.

References

1. Iler RK (1965) J Colloid Interf Sci 20:569–594
2. Decher G, Schlenhoff JB (2003) Multilayer thin films (sequential assembly of nanocomposite materials). Wiley-VCH, Weinheim
3. Lewis B, Anderson JC (1978) Nucleation and growth of thin films. Academic, New York
4. Decher G, Hong JD, Schmitt J (1992) Thin Solid Films 210:831–835
5. Lvov Y, Decher G, Möhwald H (1993) Langmuir 9:481–486
6. Decher G, Lvov Y, Schmitt J (1994) Thin Solid Films 244:772–777
7. Schmitt J, Grünewald T, Decher G, Kjaer K, Pershan PS, Lösche M (1993) Macromolecules 26:7058–7063
8. Sukhorukov GB, Möhwald H, Decher G, Lvov YM (1996) Thin Solid Films 284–285:220–223
9. Zang J, Wang Zhong-lin, Liu J, Chen S, Liu Ghang-yu (2003) Self-assembled nanostructures. Kluwer/Plenum, Dordrecht/New York
10. Crepaldi EL, Valim JB (1998) Quim Nova 21:300–311
11. Schlenoff JB, Dubas ST, Farhat T (2000) Langmuir 16:9968–9969
12. Cho J, Char K, Hong JD, Lee KB (2001) Adv Mater 13:1076–1078
13. Lee SS, Hong JD, Kim CH, Kim K, Koo JP, Lee KB (2001) Macromolecules 34
14. Chiarelli PA, Johal MS, Casson JL, Roberts JB, Robinson JM, Wang HL (2001) Adv Mater 13:1167–1171
15. Sukhorukov GB, Schmitt J, Decher G (1996) Bunsen-Ges Phys Chem 100:948–953
16. Joanny JF, Castelnovo M, Netz R (2000) Condens Matter 12:A1–A7
17. Huck WTS, Stroock AD, Whitesides GM (2000) Angew Chem Int End Engl 39:1058
18. Kalipcilar H, Gade SK, Noble RD, Falconer JL (2002) J Membr Sci 210:113–127
19. Tomita T, Nakayama K, Sakai H (2004) Micropor Mesopor Mater 68:70–75
20. Tuan VA, Li S, Falconer JL, Noble RD (2002) J Membr Sci 196:111–123
21. Arruebo M, Coronas J, Menéndez M, Santamaría J (2001) Sep Pur Tech 25:275–286
22. Kusakabe K, Kuroda T, Morooka S (1998) J Membr Sci 148:13–23
23. Menard D, Py X, Mazet N (2003) Carbon 41:1715–1727
24. Dékány I, Haraszti T (1997) Colloid Surf A 123–124:391–401
25. Kotov NA, Haraszti T, Túri L, Zavala G, Geer RE, Dékány I, Fendler JH (1997) J Amer Chem Soc 119:6821–6832
26. Haraszti T, Túri L, Dékány I, Fendler JH (1997) Models Chem 134:785–801
27. You Y, Zhao H, Vance GF (2002) Colloid Surf A 205:161–172
28. Prinetto F, Ghiotti G, Graffin P, Tichit D (2000) Micropor Mesopor Mater 39:229–247
29. Unnikrishnan R, Narayanan S (1999) J Mol Catal A 144:173–179
30. Malherbe F, Depège C, Forano C, Besse JP, Atkins MP, Sharma B, Wade SR (1998) Appl Clay Sci 13:451–466
31. Rives V (2002) Appl Clay Sci 22:75–76
32. Delcorte A, Bertrand P, Arys X, Jonas A, Wischerhoff E, Mayer B, Laschewsky A (1996) Surf Sci 366:149–165
33. Kam Sang-kyu, Gregory J (1999) Colloid Surf A 159:165–179
34. Schwarz S, Eichhorn K-J, Wischerhoff E, Laschewsky A (1999) Colloid Surf A 159:491–501
35. Schwarz S, Eichhorn KJ, Wischerhoff E, Laschewsky A (1999) Colloid Surf A 159:491–501